Virology Journal

RESEARCH

Open Access

Pathogenicity analysis of a Chinese Genogroup II Akabane virus strain (TJ2016) in mouse models

Jingjing Wang[1], Ruyang Yu[1], Fang Wei[1], Dongjie Chen[1*] and Shaoqiang Wu[1*]

Abstract

Background Akabane virus (AKAV) is divided into five genogroups (I to V), and strains of different genogroups exhibit marked differences in pathogenicity. We isolated a genogroup II AKAV strain, TJ2016, in China in 2016, but its virulence remains unknown. The pathogenic potential of other genogroup II strains isolated in China also remains uncharacterized. The objectives of this study were to determine the pathogenicity of TJ2016.

Methods Kunming or Balb/c mice at 7 days or 8 weeks of age were inoculated with TJ2016 by intracerebral (IC), intraperitoneal (IP), subcutaneous (SC), or intramuscular (IM) routes. Clinical signs, pathological alterations, and AKAV distributions in the inoculated mice were monitored and analyzed.

Results Virus inoculations by the IC route resulted in 75%~100% mortality of the inoculated mice regardless of the mouse strains or ages. Virus inoculations by the IP route killed 75% to 100% of the suckling mice but killed no adult mice. All the mice inoculated via SC and IM routes survived until the end of the trial. AKAV was detected only in the brains of the mice that died or were euthanized before the end of the experiment. The AKAV antigens were only identifiable within neuronal cells. Brain lesions such as proliferation and infiltration of microglial cells, perivascular cuffing (PVC) of lymphocytes and macrophages, neuronal degeneration/necrosis, vascular dilatation and congestion, etc., were observed only in the mice that died or were euthanized before the end of the experiment.

Conclusions We characterized the virulence of TJ2016 by inoculating suckling and adult mice via different routes and established experimental mouse models, which holds significant implications for vaccine/drug development and further research on viral pathogenesis.

Keywords Akabane virus, TJ2016 strain, Pathogenicity, Mouse model

Introduction

Akabane virus (AKAV) is an arthropod-borne virus belonging to the genus *Orthobunyavirus*, family *Peribunyaviridae*, and order *Bunyavirales* [1]. The principal vectors are *Culicoides* spp. biting midges, particularly *Culicoides brevitarsis.* As the causative agent of Akabane disease, AKAV mainly causes abortions, premature births, stillbirths, and congenital deformities such as arthrogryposis-hydranencephaly syndrome in ruminants, including cattle, sheep, goats, etc.

AKAV isolates are divided into five genogroups (I to V), and genogroup I is further subdivided into subgroups Ia and Ib [2–4]. Variant AKAV strains with variant pathogenic properties have been distributed throughout Asia, Australia, the Middle East and Africa since the prototype AKAV strain JaGAr39 was first isolated in Japan in 1959

*Correspondence:
Dongjie Chen
chendongjie1212@163.com
Shaoqiang Wu
sqwu@sina.com
[1] Institute of Animal Inspection and Quarantine, Chinese Academy of Quality and Inspection & Testing, Beijing 100176, China

[5]. AKAV belonging to genogroups II, III, and V primarily cause congenital abnormalities in the fetus, while strains in genogroup I cause postnatal encephalomyelitis with neurological disorders [6]. The genogroup Ia strain Iriki, which was isolated in Japan in 1984, caused nonsuppurative encephalitis and neurological signs in calves [7]. Since then, AKAV strains that caused encephalomyelitis in calves and adult cattle were reported in Japan [8, 9] and South Korea [10, 11]. The pathogenicity of the genogroup IV strains isolated in Africa was unknown [12].

The pathogenicity of the AKAV strains has been extensively studied in animal models. AKAV-7, one of the fifteen strains isolated from the affected cows in a major outbreak of encephalomyelitis in Korea in 2010, was classified into genogroup Ia within the Iriki strain. The neuropathogenicity of AKAV-7 causing encephalomyelitis was verified by experimental infection in six-month-old female cows [13] and adult goats [14] through various inoculation routes. Pathogenicity of strains Iriki [7] and OBE-1 [15], as representative strains from genogroups I and II, respectively, were frequently analyzed and compared in mouse models [16–18]. In general, Iriki is more virulent than OBE-1 in mice, as it is in cattle.

In 2016, an AKAV strain defined as TJ2016 was first isolated from bovine sera in China [19]. The cattle in the herd showed no symptoms at that time and were likely just virus carriers. However, the TJ2016 strain was closely related to the AKAV strain JaGAr39, which was classified into genogroup II and was found to be fatally virulent to suckling and adult mice [5]. The goal of this work was to determine the pathogenicity of the TJ2016 strain to give insight into the virulence of genogroup II AKAV strains isolated in China.

Materials and methods

Cells, antibodies, and virus

BHK-21 cells were stored in our laboratory (the Institute of Animal Inspection and Quarantine, Chinese Academy of Quality and Inspection & Testing) and maintained at 37℃ in 5% CO_2 in Dulbecco's minimal essential medium (DMEM; Gibco) containing 10% heat-inactivated fetal bovine serum (FBS; Gibco).

The mouse monoclonal antibody (mAb) 2D3 specific to AKAV N protein and the rabbit polyclonal antibody (pAb) specific to AKAV were both prepared in our laboratory previously [20]. FITC-labeled goat anti-mouse IgG and HRP-conjugated goat anti-mouse IgG were purchased from SolarbioLife Sciences (Beijing, China).

The TJ2016 strain of AKAV (GenBank accession no. MT761689, MT761688, and MT755621) was isolated and stored by our lab [19]. TJ2016-F6 was derived from TJ2016 by serial passaging in BHK-21 cells for six rounds. The virus titers were determined by a microtitration infectivity assay in BHK-21 cells after removal of cell debris by centrifugation and recorded as 50% tissue culture infective doses ($TCID_{50}$) per milliliter.

Animals

Eight-week-old female Balb/c mice and Kunming mice, as well as 7-day-old Balb/c mice and Kunming mice, were purchased from Beijing Vital River Laboratory Animal Technology Co., Ltd. All the mice used in this experiment were specific pathogen-free (SPF).

Animal trials

To analyze the pathogenicity of TJ2016 in suckling Kunming mice, 7-day-old Kunming mice were inoculated with 10^4 $TCID_{50}$ to 10^5 $TCID_{50}$ of TJ2016 or an equal volume of DMEM containing 2% FBS by intracerebral (IC), intraperitoneal (IP), subcutaneous (SC), or intramuscular (IM) routes, respectively. Details of the experiments are summarized in Table 1. Clinical signs, body weight, and survival of each mouse were monitored for 7 days, and the surviving mice were euthanized at the end of the experiment. A clinical sign scoring system was established in this study (Table 2), and a score of clinical signs was given to each mouse. Six organs, including the brain, heart, liver, spleen, lung, and kidney, were collected from each mouse for further analysis.

The pathogenicity of TJ2016 was also evaluated using the same processes in 8-week-old female Kunming mice, 7-day-old Balb/c mice, and 8-week-old female Balb/c mice. In this part of the animal trail, the mice were challenged via IC and IP routes, and only brain tissue samples were collected from each mouse. Four mice were used in each AKAV-inoculated group, and two mice were used in each negative group. The challenge dose for adult

Table 1 Inoculation of the 7-day-old Kunming mice by different routes

Inoculation route	Group name	Inoculum	Number of mice	$TCID_{50}$ per mouse
IC	KM-7d-IC	AKAV	6	10^4
	DMEM-IC	2% DMEM	3	/
IP	KM-7d-IP	AKAV	6	10^5
	DMEM-IP	2% DMEM	3	/
SC	KM-7d-SC	AKAV	6	10^5
	DMEM-SC	2% DMEM	3	/
IM	KM-7d-IM	AKAV	6	10^5
	DMEM-IM	2% DMEM	3	/

IC intracerebral, *IP* intraperitoneal, *SC* subcutaneous, *IM* intramuscular, *KM* Kunming mice, *7d* 7-day-old, *2% DMEM* DMEM with 2% FBS and penicillin (50 U/mL)-streptomycin (50 mg/mL)

Table 2 Clinical sign scoring system used for the mice inoculated with AKAV

	Symptom type	Standard for evaluation	Score
GCS	Appetite	Normal	0
		Inappetence	1
	Mental state	Normal	0
		Lethargy/ disorientation/ coma	1
	Coat condition	Normal	0
		Ruffled	1
NSS	Nervous signs	Normal	0
		Tremors	1
		Ataxia	2
		Paddling movements	3
		Paralysis	4

GCS gross clinical score, *NSS* nervous signs score, *total score* GCS + NSS

If the mouse died, total score = 10; 0 ≤ total score ≤ 10

Table 3 Mortality of Kunming and Balb/c mice inoculated by TJ2016

Group (Mouse-age-route)	$TCID_{50}$ per mouse		
	10^4	10^5	10^6
KM-7d-SC	N/A	**0/6**	N/A
KM-7d-IM	N/A	**0/6**	N/A
KM-7d-IP	N/A	**6/6**	N/A
KM-7d-IC	**6/6**	N/A	N/A
KM-8w-IP	N/A	N/A	**0/4**
KM-8w-IC	N/A	N/A	**3/4**
Balb/c-7d-IP-1	N/A	**0/4**	N/A
Balb/c-7d-IP-2	N/A	N/A	**3/4**
Balb/c-7d-IC	**4/4**	N/A	N/A
Balb/c-8w-IP	N/A	N/A	**0/4**
Balb/c-8w-IC	N/A	N/A	**4/4**

IC intracerebral, *IP* intraperitoneal, *SC* subcutaneous, *IM* intramuscular, *KM* Kunming mice, *7d* 7-day-old, *8w* 8-week-old, *N/A* not applicable

mice was set directly at the maximum level (10^6 $TCID_{50}$ per mouse), while the dose for 7-day-old Balb/c mice was determined based on that used for 7-day-old Kunming mice. Since the 10^5 $TCID_{50}$ per mouse dose did not cause mortality in Balb/c suckling mice via IP inoculation, an additional challenge group with 10^6 $TCID_{50}$ per mouse was included. Detailed information was summarized in Table 3. Mice with severe paralysis were considered and recorded as dead and were euthanized.

RNA extraction and RT-PCR amplification

RNA of the collected tissue samples was extracted using the RNA Easy Fast Tissue/Cell Kit (TianGen Biotech, Beijing, China) according to the manufacturer's instructions. To determine the presence of AKAV RNA in different organs, we performed RT-PCR assays targeting the AKAV N gene using previously published primers (N-F2: cgatgttccacaacggaatg; N-R2: aagctctagctgcaggtgag) [21]. The extracted RNA was amplified by using the HiScript II One Step RT-PCR Kit (Vazyme, Nanjing, China) in the following process: 50℃ for 30 min; 94℃ for 3 min; 35 cycles of denaturation at 94℃ for 30 s, annealing at 55℃ for 30 s, and extension at 72℃ for 1 min/kb; 72℃ for 5 min and hold at 4℃. The RNA extracted from the AKAV-infected BHK-21 cells and ddH_2O served as the positive control and negative control, respectively. All the PCR products were examined by gel electrophoresis.

Virus titration and immunofluorescence assay (IFA)

The brain tissues were suspended in DMEM to a concentration of 10% and ground thoroughly. Resulting homogenates were centrifuged at 12,000 rpm for 15 min at 4℃. The supernatant was collected for determination of viral titers by a microtitration infectivity assay in BHK-21 cells. Briefly, confluent monolayers of BHK-21 cells cultured in 96-well plates were incubated with ten-fold serially diluted supernatant of the brain homogenate. After absorption for 2 h at 37 °C with 5% CO_2, the supernatant was removed and changed with DMEM supplemented with 2% FBS and 200 U/mL of penicillin–streptomycin. The plates were incubated for an additional 48 h at 37 °C with 5% CO_2. After 48 h of incubation, the supernatant was removed and the cells were fixed with pre-cooled absolute ethyl alcohol for 30 min. MAb 2D3 was used as the primary antibody, and the FITC-labeled goat anti-mouse IgG was used as the secondary antibody. Fluorescence images were observed and obtained by the Invitrogen EVOS FL cell fluorescence imaging system (Thermo Fisher Scientific, Waltham, USA). Viral titers were determined and recorded as $TCID_{50}$ per gram according to the Reed-Muench method [22].

Histopathology examination

Half of the collected brain from each mouse was fixed in 4% paraformaldehyde for 48 h and then sent to Bioss (Beijing, China) to be embedded in paraffin wax and sectioned for hematoxylin and eosin (HE) staining and immunohistochemistry (IHC) examination. For the IHC assay, the rabbit pAb (1:1000 dilutions) specific to AKAV was used as the primary antibody, and the goat anti-rabbit IgG H&L (HRP polymer) (Bioss, Beijing, China) was used as the secondary antibody.

Brain sections stained with HE were evaluated, and scores from 0 to 4, which accounted for the distribution and severity of the microscopic lesions, were recorded. The indications for the scores were as follows: 0 = no microscopic lesions, 1 = mild microscopic lesions,

2 = moderate multifocal microscopic lesions, 3 = moderate diffuse microscopic lesions, and 4 = severe microscopic lesions. The detection of the AKAV antigen was executed through a ranked score of 0 to 4, which was used to evaluate the number of positive cells per section. The indications for the scores were as follows: 0 = no positive cells, 1 = 1–10 positive cells/section, 2 = 11–30 positive cells/section, 3 = 31–100 positive cells/section, and 4 = > 100 positive cells/section.

Phylogenetic analyses

The open reading frame (ORF) sequences of the S and M segments of the reference AKAV strains were downloaded from GenBank. Detailed information on these strains was shown in Table 4. The sequences were aligned using the ClustalW algorithm in MEGA 7.0. A phylogenetic tree was then constructed based on the maximum likelihood method. To assess the robustness of the tree topology, we performed 100 bootstrap replicates, with the bootstrap values calculated from the resulting consensus tree.

Statistical analysis

The data were analyzed using GraphPad Prism version 8.0 software (GraphPad Software, USA). Differences between groups were analyzed by using two-way analysis of variance (ANOVA) with Geisser-Greenhouse correction. A two-tailed unpaired t-test with Welch's correction was used to estimate the significance of the virus titers. Error bars represent the standard deviations (SD), as indicated in the figure legends. Differences were considered statistically significant at a P value of < 0.05 and extremely significant at a P value of < 0.01 or < 0.001 or < 0.0001.

Table 4 Information of AKAV reference strains

AKAV Strain	Year	Country	Genogroup	Accession No	
				S CDS	M CDS
Iriki	1984	Japan	I	AB289321.1	AB297820.1
OBE-1	1974	Japan	II	AB000851.1	AB100604.1
Okayama2001	2001	Japan	I	AB289319.1	AB289322.1
Okayama2004	2004	Japan	II	AB289320.1	AB289323.1
AKAV-7/SKR/2010	2010	Korea	I	JQ308771.1	JQ308775.1
CX-01	2019	China	I	MW194117.1	MW194115.1
JaGAr39	1959	Japan	II	AB000852.1	AB297818.1
JaLAB39	1959	Australia	II	KR260714.1	KR260715.1
CQ/AKAV-1/2023	2023	China	II	OR791102.1	OR791103.1
TJ2016	2016	China	II	MT755621.1	MT761688.1

CDS coding sequence

Results

The TJ2016 strain exhibits lethal virulence in Kunming suckling mice through both IC and IP routes of inoculation

To study the pathogenicity of AKAV strain TJ2016, we inoculated the 7-day-old Kunming mice by IC, IP, SC, and IM routes (Table 1). The inoculated mice in the KM-7d-IM group, KM-7d-SC group, and the control groups all survived during the 7-day observation period and presented no clinical symptoms. The six mice inoculated by the IC route all died at 3 days post inoculation (dpi). In the KM-7d-IP group, one mouse died at 3 dpi, four mice died at 4 dpi, and one mouse died at 6 dpi (Fig. 1A). Neurological symptoms such as tremors, ataxia, paddling movements, or paralysis were observed in the mice inoculated via IC and IP routes before death (Fig. 1B). The average daily weight gain (ADWG) of mice in each group was calculated. As Fig. 1C showed, weight loss was observed in mice of both the KM-7d-IC group and the KM-7d-IP group, which is consistent with the mortality. The ADWG of the mice inoculated by IC route at 1 ~ 3 dpi and the ADWG of the mice inoculated by IP route at 3 ~ 4 dpi were significantly reduced compared to those of the control groups (Fig. 1C).

Distribution of AKAV in the inoculated mice

To determine the viral tissue tropism of AKAV in the inoculated mice, the AKAV N gene in organs including the brain, heart, liver, spleen, lung, and kidney of each mouse was detected by the RT-PCR method. As a result, positive bands with 649 bp were only observed in the brains of the mice from the KM-7d-IC and KM-7d-IP groups (Fig. 2). The genome of AKAV was not detected in any organs of the mice in the KM-7d-SC and KM-7d-IM groups, which indicated that the AKAV strain TJ2016 failed to infect the 7-day-old Kunming mice by SC or IM routes.

Brain lesions and IHC examinations

Gross tissue lesion examinations were carried out immediately after the mice died or at the end of the experiment. The brains of the mice that died or were euthanized before the end of the experiment in the KM-7d-IC group exhibited severe edema, hemorrhage, and liquefaction (Fig. 3A). Mild brain lesions, such as localized hemorrhage and brain tissue softening, were observed in the mice that died or were euthanized before the end of the experiment in the KM-7d-IP group (Fig. 3A). All the brains of the mice in the other two inoculated groups (data not shown) and the control groups display no gross lesions (Fig. 3A).

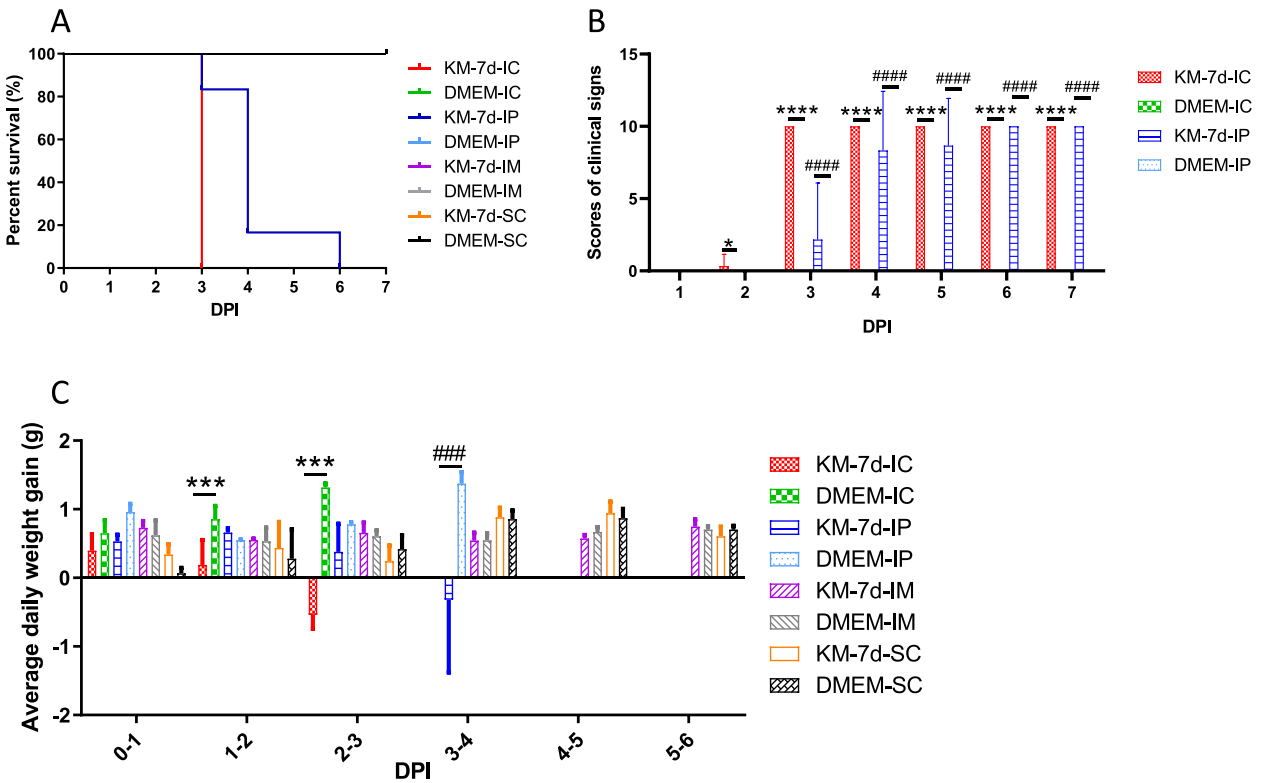

Fig. 1 Survival curve of the 7-day-old Kunming mice inoculated with TJ2016 by different routes. **A** Survival curves of the mice in different groups. **B** Average clinical scores of the mice in different groups. **C** ADWG of the mice in different groups. The data are shown as means ± SD (error bars). Statistical differences are labeled according to two-way analysis of variance with Geisser-Greenhouse correction. Asterisks (*) indicate a significant difference between the KM-7d-IC and DMEM-IC groups (*, $P < 0.05$; ***, $P < 0.001$; ****, $P < 0.0001$). Pounds (#) indicate a significant difference between the KM-7d-IP and DMEM-IP groups (###, $P < 0.001$; ####, $P < 0.0001$). IC, intracerebral; IP, intraperitoneal; SC, subcutaneous; IM, intramuscular; KM, Kunming mice; 7d, 7-day-old; DPI, days post inoculation

According to the PCR result, the AKAV antigen distribution in the AKAV-positive brains was further examined by IHC analysis, and the microscopic brain lesions were further observed after HE staining. Brains of mice in the control group were used as the negative control. Immunohistochemical staining showed that viral antigens were present in the neurons throughout the brains of the mice that died or were euthanized before the end of the experiment, and the scores of the antigens in both groups were equal (Fig. 3B, Table 5). The brains of the mice inoculated by the IC route exhibited severe histopathological changes characterized by perivascular cuffing (PVC) of lymphocytes and macrophages, neuronal degeneration and necrosis, glial nodules (GN) consisting of microglial cells (gliosis), and tissue liquefaction with loose structure. Meanwhile, PVC of lymphocytes and macrophages and GN consisting of microglial cells were also observed in the brains of the mice inoculated by the IP route. Overall severity of the microscopic brain lesions in the KM-7d-IC group was greater than that in the KM-7d-IP group (Fig. 3C, Table 5).

Virus load in the infected mice

In order to detect infectious AKAV virions in the brain tissue and quantify the viral load, the tissue was homogenized, followed by IFA and microtitration infectivity assay on the homogenate. The results showed that AKAV virus particles with infectious activity could be detected in both the IC and the IP groups (Fig. 4A). The average virus titers in brains of the IC group ($10^{8.2}$ $TCID_{50}$/g) were higher than those of the IP group ($10^{8.0}$ $TCID_{50}$/g) with no significant difference (Fig. 4B).

The effects of mouse strain and age on the pathogenicity of TJ2016

To investigate the effects of mouse strain and age on the pathogenicity of the TJ2016 strain, we inoculated 8-week-old Kunming mice, 7-day-old Balb/c mice, and 8-week-old Balb/c mice with the TJ2016 strain by IC and IP routes (Table 3).

All the 7-day-old Balb/c mice inoculated by the IC route died before the end of the experiment (Table 3, Fig. 5A). While for the 7-day-old Balb/c mice inoculated

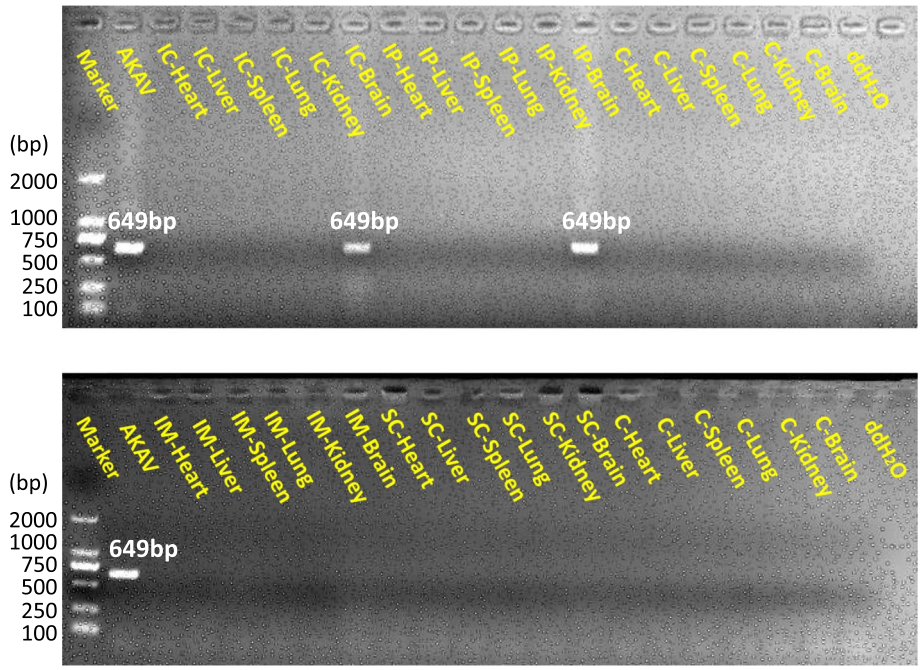

Fig. 2 RT-PCR detection of the AKAV N gene in organs collected from the inoculated mice. RT-PCR testing was performed on all collected tissues from each inoculated mouse, but only the results from one mouse of each group are shown as representative. The RNA extracted from the AKAV-infected BHK-21 cells was used as the positive control, and the ddH_2O was used as the negative control. IC, intracerebral; IP, intraperitoneal; SC, subcutaneous; IM, intramuscular; C, control. For example, IC-heart indicates the heart tissue from the mouse inoculated by the IC route, and C-brain indicates the brain tissue from the mouse in the control group

by IP route, all the mice survived when the inoculation dose was 10^5 $TCID_{50}$ per mouse, and 75% (3/4) of the mice died when the inoculation dose was raised to 10^6 $TCID_{50}$ per mouse (Table 3, Fig. 5A). Through the whole duration of the experiment, all the 8-week-old mice inoculated by the IP route survived regardless of the mouse strain (Kunming or Balb/c) (Table 3, Fig. 5B and C). While for the 8-week-old mice inoculated by the IC route, a 75% (3/4) mortality rate was found in the Kunming mice and a 100% (4/4) mortality rate was found in the Balb/c mice (Table 3, Fig. 5B and C). Neurological symptoms such as tremors, ataxia, paddling movements, or paralysis were observed in all the mice that died or were euthanized before the end of the experiment (Fig. 5D, E, and F). Obvious negative ADWG was observed in groups Balb/c-7d-IC (3 ~ 4 dpi), Balb/c-8w-IC (0 ~ 5 dpi), and KM-8w-IC (0 ~ 3 dpi). While the ADWG of the other groups showed no significant difference with that of the control groups (Fig. 5G, H, and I).

The brains of each mouse from all the groups were collected for AKAV detection. RT-PCR results showed an interesting pattern—all the mice that died or were euthanized before the end of the experiment in each group had the AKAV genome in their brains (Fig. 6A), whereas all the mice surviving until the end of the experiment were negative (Fig. 6B). The viral loads of these AKAV-positive brains were determined, and the average titers ranged from $10^{5.2}$ $TCID_{50}$/g to 10^7 $TCID_{50}$/g. In general, suckling mice exhibited higher viral loads in brain tissues than adult mice. Significant or extremely significant differences were observed in each of the two groups (Fig. 6C).

Consistent with the PCR results, the brain tissues of the mice that died or were euthanized before the end of the experiment in groups KM-8w-IC, Balb/c-8w-IC, Balb/c-7d-IC, and Balb/c-7d-IP-2 showed high levels of AKAV antigens (Fig. 7A, B, and C, Table 5) and notable pathological changes (Fig. 7D, E, and F). It is noteworthy that there were certain differences in brain tissue lesions among these mice. The main histopathological feature of the brain tissues in group KM-8w-IC was proliferation and infiltration of microglial cells. Occasional vascular dilatation and congestion and neuronal degeneration/necrosis were also found in this group (Fig. 7D). The histopathological changes in group Balb/c-8w-IC were characterized by multifocal vascular dilation and congestion, localized brain tissue liquefaction, and partial neuronal necrosis (Fig. 7E). The most severe brain lesion was observed in mice from groups Balb/c-7d-IC and Balb/c-7d-IP-2, which exhibited complete disappearance of brain structure, hemorrhage, and multifocal infiltration of microglial cells (Fig. 7F). Microscopic brain lesion scores of the mice in different groups were summarized

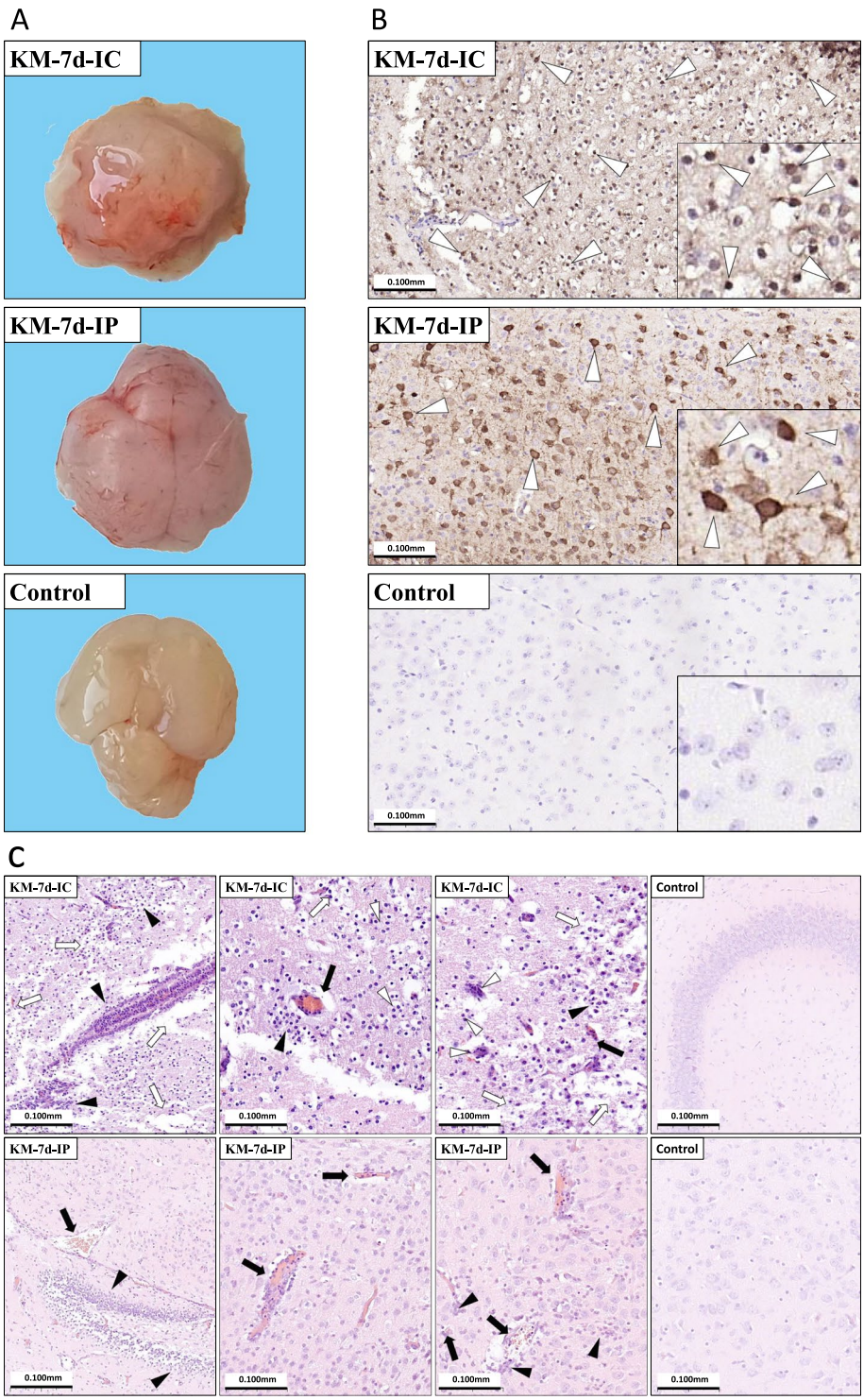

Fig. 3 Brain lesions and IHC examinations of the 7-day-old Kunming mice inoculated with TJ2016. **A** Gross brain lesions. **B** IHC examinations for AKAV antigen. The neuron stained intensely dark brown, representing AKAV antigen-positive cells. Hollow triangles indicate positive signals. **C** Microscopic brain lesions stained with HE. Solid arrows indicate PVC of lymphocytes and macrophages. Hollow arrows indicate tissue liquefaction with loose structure. Solid triangles indicate GN consisting of microglial cells. Hollow triangles indicate neuronal degeneration or necrosis. KM, Kunming mice; 7d, 7-day-old; IC, intracerebral; IP, intraperitoneal

Table 5 The histopathology results of the inoculated mice in different groups

Group (Mouse-age-route)	IHC score		Microscopic brain lesion score	
	Dead mice	Survived mice	Dead mice	Survived mice
KM-7d-IP	4	N/A	3	N/A
KM-7d-IC	4	N/A	4	N/A
KM-8w-IP	N/A	0	N/A	0
KM-8w-IC	4	N/A	2.3	N/A
Balb/c-7d-IP-2	4	N/A	4	N/A
Balb/c-7d-IC	4	N/A	4	N/A
Balb/c-8w-IP	N/A	0	N/A	0
Balb/c-8w-IC	4	N/A	3.3	N/A

IHC scores: 0 = negative; 1 = 1–10 positive cells/section; 2 = 11–30 positive cells/section; 3 = 31–100 positive cells/section; 4 = > 100 positive cells/section

Microscopic brain lesion scores: 0 = no microscopic lesions; 1 = mild microscopic lesions; 2 = moderate multifocal microscopic lesions; 3 = moderate diffuse microscopic lesions; 4 = severe microscopic lesions. The IHC scores and the microscopic brain lesion scores are both averaged from three tissue sections

IHC immunohistochemistry, *Dead mice* the mice that died or were euthanized before the end of the experiment; Survived mice, the mice that survived until the end of the experiment, *IC* intracerebral, *IP* intraperitoneal, *KM* Kunming mice, *7d* 7-day-old, *8w* 8-week-old, *N/A* not applicable (no mice were present/analyzed in these groups)

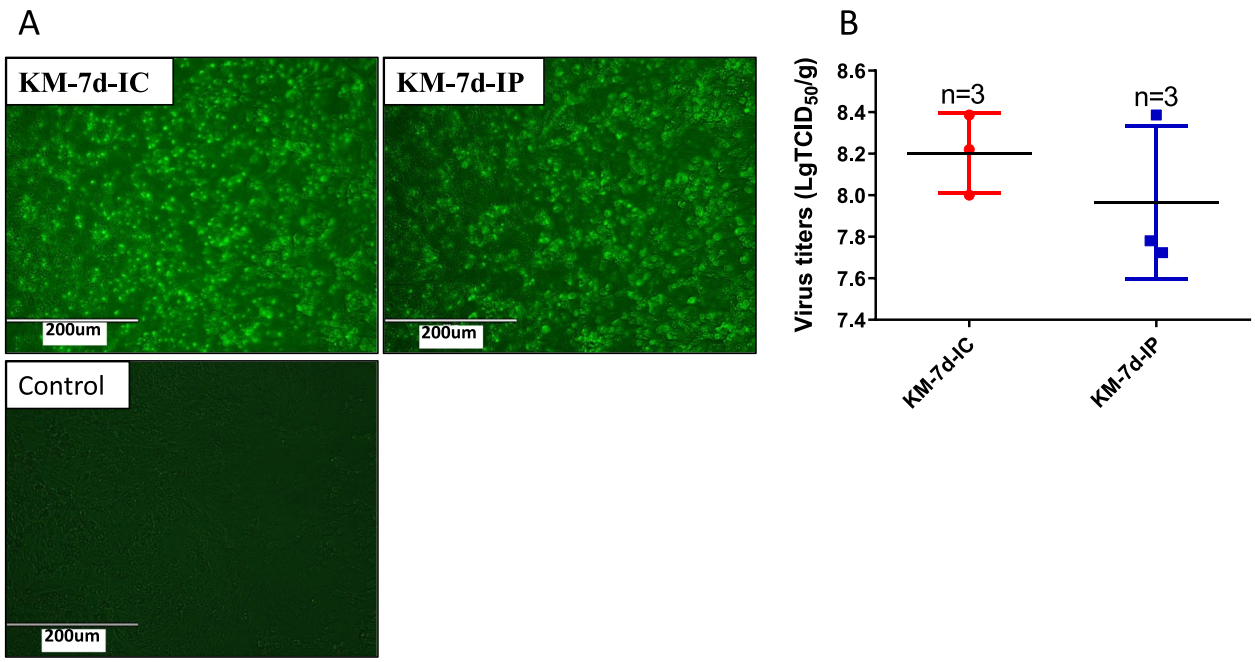

Fig. 4 Determination of the infectious AKAV in brains of the 7-day-old Kunming mice inoculated with TJ2016. Virus titers in brain tissue homogenates from the KM-7d-IC and KM-7d-IP groups were determined by microtitration infectivity assay and IFA assay in BHK-21 cells. **A** IFA detection of the AKAV N protein. The fluorescence images were obtained from the wells inoculated by the 10^4-fold diluted homogenates. **B** Virus titers in brains of each group. The data are shown as means ± SD (error bars) from three independent experiments. KM, Kunming mice; 7d, 7-day-old; IC, intracerebral; IP, intraperitoneal

in Table 5. Generally, the mice in the Balb/c-7d-IC and Balb/c-7d-IP-2 groups showed higher scores than those in the Balb/c-8w-IC group, which in turn showed higher scores than those in the KM-8w-IC group (Table 5). The mice surviving until the end of the experiment in the other groups showed neither detectable antigens (Fig. 7A, B, and C) nor any histopathological changes (Fig. 7D, E, and F).

Phylogenetic analysis

The phylogenetic trees were constructed to clarify the genetic relationships between TJ2016 and the other

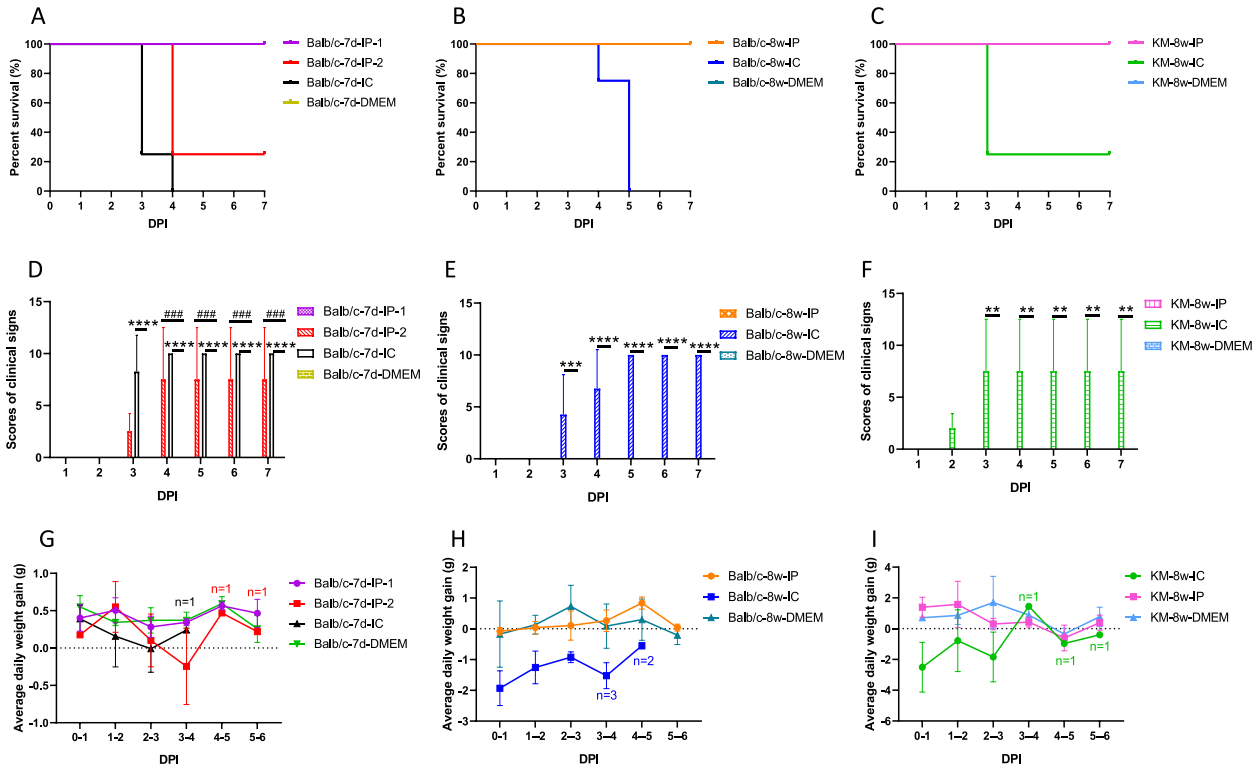

Fig. 5 Survival curve of the inoculated mice of different mouse strains and ages. **A**, **B**, and **C** Survival curves of the mice in different groups. **D**, **E**, and **F**) Average clinical scores of the mice in different groups. **G**, **H**, and **I**) ADWG of the mice in different groups. The data are shown as means ± SD (error bars). Asterisks (*) indicate a significant difference between the Balb/c-7d-IC and Balb/c-7d-DMEM groups, or between the Balb/c-8w-IC and Balb/c-8w-DMEM groups, or between the KM-8w-IC and KM-8w-DMEM groups (**, $P < 0.01$; ***, $P < 0.001$; ****, $P < 0.0001$). Pounds (#) indicate a significant difference between the Balb/c-7d-IP-2 and Balb/c-7d-DMEM groups (###, $P < 0.001$). IC, intracerebral; IP, intraperitoneal; KM, Kunming mice; 7d, 7-day-old; 8w, 8-week-old; DPI, days post inoculation

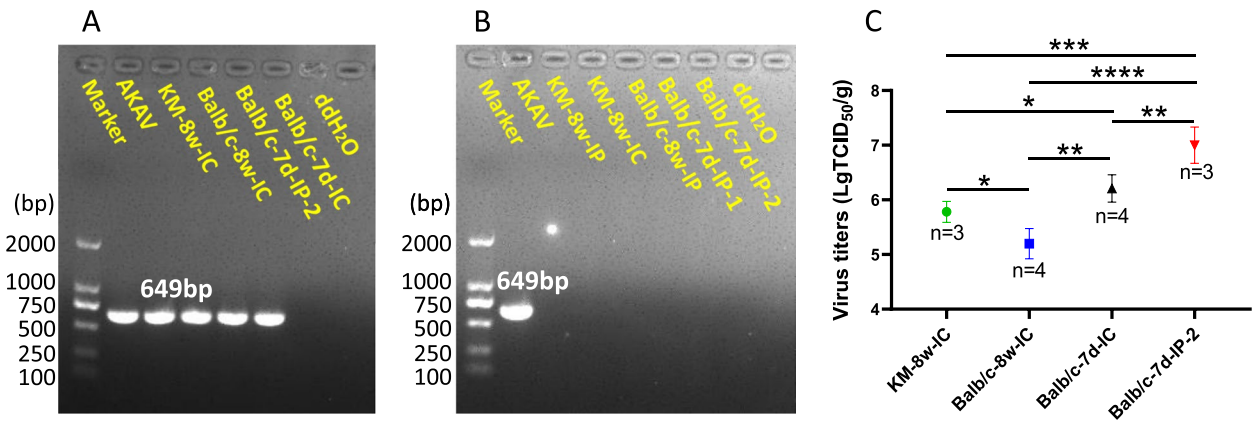

Fig. 6 Detection of AKAV in brains of the inoculated mice of different mouse strains and ages. RT-PCR testing was performed on all tissues from the mice that died or were euthanized before the end of the experiment (**A**) and the mice surviving until the end of the experiment (**B**). Virus titers in brains of the mice that died or were euthanized before the end of the experiment were measured (**C**). The data are shown as means ± SD (error bars) from three independent experiments. Statistical differences are labeled according to a two-tailed untailed t-test with Welch's correction. Asterisks indicate significant differences between any two groups (*, $P < 0.05$; **, $P < 0.01$; ***, $P < 0.001$; ****, $P < 0.0001$). IC, intracerebral; IP, intraperitoneal; KM, Kunming mice; 7d, 7-day-old; 8w, 8-week-old

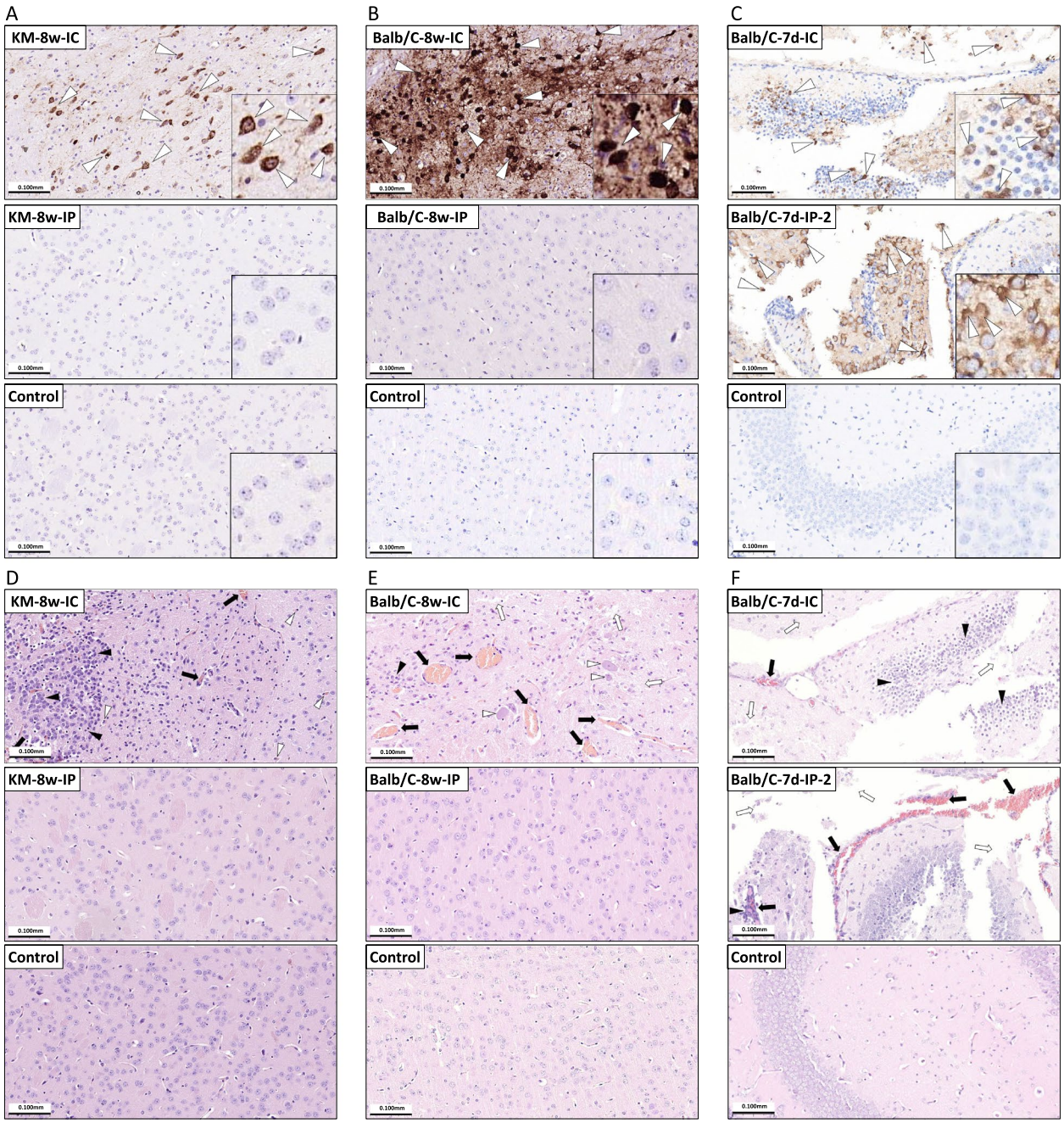

Fig. 7 Microscopic brain lesions and IHC examinations of the inoculated mice of different strains and ages. **A**, **B**, and **C** IHC examinations for AKAV antigen. The neuron stained intensely dark brown, representing AKAV antigen-positive cells. Hollow triangles indicate positive signals. **D**, **E**, and **F** Microscopic brain lesions stained with HE. Solid arrows indicate vascular dilatation, congestion, hemorrhage, or PVC of lymphocytes and macrophages. Hollow arrows indicate brain tissue liquefaction with loose structure or disappearance of brain structure. Solid triangles indicate proliferation and infiltration of microglial cells. Hollow triangles indicate neuronal degeneration or necrosis. IC, intracerebral; IP, intraperitoneal; KM, Kunming mice; 7d, 7-day-old; 8w, 8-week-old

reference AKAK strains. The reference strains CQ/AKAV-1/2023, JaGAr39, and JaLAB39 show high similarity to TJ2016 in genetics. The other reference strains were selected for the reason that their pathogenicity has been studied in animal models. According to the phylogenetic trees, whether based on the coding sequence (CDS) of S segment N protein (Fig. 8A) or M segment (Fig. 8B), all the selected reference strains are segregated

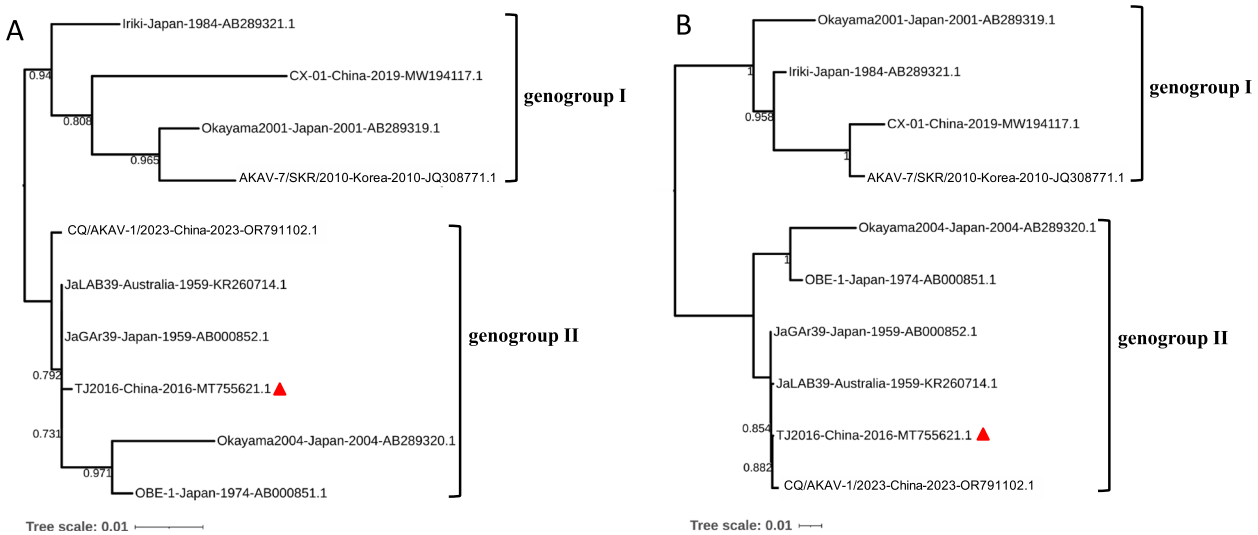

Fig. 8 Molecular phylogenetic analysis by maximum likelihood method. Phylogenetic trees of AKAV based on the coding sequence (CDS) of the S segment of N protein (**A**) and M (**B**) segments. Branch lengths are proportional to the number of nucleotide substitutions per site. Bootstrap values were determined from 1000 bootstrap iterations, and only the values higher than 0.7 were shown. The TJ2016 strain used in this study was indicated by red triangles

into genogroup I and genogroup II, and TJ2016 is classified within genogroup II. The phylogenetic analysis of the N protein (Fig. 8A) showed that the TJ2016 is clustering closely with strains JaGAr39 (isolated in Japan, 1959) and JaLAB39 (isolated in Australia, 1959). While TJ2016 is most closely related to strains JaLAB39 and CQ/AKAV-1/2023 (isolated in China, 2023) when the M segment was phylogenetically analyzed (Fig. 8B).

Discussion

Most of the AKAV strains isolated in China belong to genogroup Ia [3, 23], and one of the representative strains, CX-01, has been studied for pathogenicity using a mouse model [24]. Following the isolation of TJ2016 in China in 2016, CQ/AKAV-1/2023 was isolated in China in 2023. Both strains cluster within genogroup II and exhibit high genetic identity to the classical strain JaGAr39 (Table 4, Fig. 8), confirming the presence of genogroup II AKAV in China's livestock. In this present study, we investigated the pathogenicity of the Chinese genogroup II strain TJ2016 by studying clinical and histopathological responses in mice (with different mouse strains and ages) following the inoculation of this isolate by different routes.

In the 7-day-old Kunming mice infection model, IC and IP inoculations resulted in a 100% (6/6, 6/6) mortality rate, while IM and SC inoculations caused no death (Fig. 1A). IP and IC were also the most commonly used routes in previous studies regarding AKAV infection [16–18, 24, 25]. Therefore, we next inoculated the 8-week-old Kunming mice, 7-day-old Balb/c mice, and 8-week-old Balb/c mice by IC and IP routes. According to the mortality summarized in Table 3, we found that TJ2016 exhibited higher lethality in suckling mice compared to adult mice regardless of the inoculation routes and mouse strains, higher lethality by IC inoculation than IP inoculation regardless of the mouse strains, and higher lethality in suckling Kunming mice compared to suckling Balb/c mice by IP inoculation route. As expected, a higher challenge dose can also increase the mortality. Taken together, the fatal virulence of TJ2016 was affected by the inoculation route, challenge dose, mouse strain, and age. It should be noted that all of the 8-week-old mice inoculated via the IP route survived to the trial termination irrespective of mouse strains. The fatal virulence of TJ2016 diminishes with age, which might be associated with the progressive maturation of the blood–brain barrier (BBB) during murine adulthood [17, 26].

The tissue tropism of TJ2016 in the infected suckling Kunming mice was analyzed. RT-PCR results revealed that TJ2016 selectively infected brain tissue, with no detectable infection in the heart, liver, spleen, lungs, or kidneys. The other AKAV strains (such as Iriki, OBE-1, and AKAV-7/SKR/2010) were reported to be able to infect the other tissues, including the spinal cord, spleen, thymus, lymph nodes, heart, liver, lungs, kidneys, and small intestine of the inoculated mice in the other studies [17, 18, 25]. Besides, we found that the virus was only detected in the brains of the mice that died or were euthanized before the end of the experiment, whereas it was

not observed in the mice surviving until the end of the experiment, suggesting a correlation between virus replication efficiency in the brain and the fatal virulence in mice, which is consistent with a previous study [27]. The IHC assay showed that TJ2016 demonstrated selective tropism for neurons within cerebral tissues, aligning with established findings in prior research [13, 17, 24, 25, 27].

As the first described genogroup II AKAV strain, JaGAr39 was found to be fatally virulent to the DD strain of albino mice by the IC route, which can kill the inoculated suckling (2 ~ 4 days old) and adult mice (4 weeks old) following the minimum incubation period of 2 and 3 days [5]. OBE-1 is a classic representative strain of genogroup II AKAV. Ogawa et al. reported that all of the suckling Balb/c mice inoculated with OBE-1 by IP route survived during the 21-day observation period [16]. Similarly, Takenaka-Uema et al. also reported that OBE-1 caused no mortality and no remarkable clinical signs in the suckling BALB/cCrSlc mice when challenged by the IP route [18]. Murata et al. inoculated the BALB/cAJcl mice from 3 days to 8 weeks of age by IP or IC routes with OBE-1 and found that only the 3-day-old mice inoculated by the IC route showed mild brain lesions, indicating that both neuroinvasiveness and neurovirulence of the OBE-1 strain diminish with age [17]. While the Iriki strain, a classic representative strain of genogroup I AKAV, can kill both the suckling and adult Balb/c mice and can cause severe brain lesions in the infected mice [16–18]. The OBE-1 strain results mainly in abortions and congenital abnormalities by infection of fetuses but does not cause any apparent lesions in postnatal animals [28]. While the Iriki strain is more virulent and causes non-suppurative encephalomyelitis in newborn cattle [7]. These findings collectively demonstrate a positive correlation between the pathogenic potential of AKAV strains in bovine and murine hosts. It can be inferred that the TJ2016 strain, which demonstrated lethal virulence and caused severe brain lesions in mice in this study, may similarly possess high virulence in cattle, with the potential to induce abortions and congenital abnormalities in fetuses and non-suppurative encephalomyelitis in newborn cattle, suggesting its potential threat to China's livestock industry.

Suckling Balb/c mice have been widely utilized in neurovirulence studies of AKAV [17, 18, 29]. While it is challenging to collect blood samples from suckling mice for viremia studies, and the short lifespan of suckling mice is insufficient for observing immune responses, limiting its application in vaccine studies. Type I interferon receptor knockout (IFNAR1 KO) mice were susceptible to viral infection and have been used to study infection, disease, pathogenesis, and vaccine testing against multiple arbovirus families such as Bunyaviridae, Togaviridae, Flaviviridae, Rhabdoviridae, Orthomyxoviridae, and Reoviridae [30]. Since Schmallenberg virus (SBV), a Simbu serogroup virus with pathological findings similar to those of AKAV infection in ruminants [31], was found to have fatal virulence to adult IFNAR1 KO mice but not to adult C57BL/6 mice [32], IFNAR1 KO mice were used as an animal model of SBV vaccine studies [33, 34]. A recent study reported that IFNAR1 KO mice were also a good choice for assessing AKAV pathogenicity and vaccine efficacy [35]. However, employing IFNAR1 KO mice is often prohibitively expensive and limited by funding constraints. In this study, both BALB/c and Kunming mice are commonly used and cost-effective strains, with certain differences in body size. We found that infection of the TJ2016 strain by the IC route could induce the brain lesions and death of both adult BALB/c and adult Kunming mice. After optimizing the challenge dose, this model could serve as a viable alternative to IFNAR1 KO mice for AKAV vaccine research. The study's limitations were that the collection and analysis of samples were not comprehensive enough, such as the spinal cord, thymus, blood, and lymph nodes were not collected due to the extensive workload involved in this study. Additionally, this study only preliminarily explored the lethal dose of TJ2016 in mice but did not accurately determine the LD50, as it would require sacrificing too many animals, which would contradict animal welfare principles.

Conclusion

This study describes the pathogenicity of TJ2016, a Chinese genogroup II AKAV strain, in mice of different mouse strains and different ages infected via various challenge routes. In conclusion, TJ2016 exhibited lethal virulence in both adult and suckling Kunming mice and Balb/c mice when inoculated via the IC route. However, IP inoculation of TJ2016 caused lethal infection in suckling mice of both Kunming and Balb/c strains but failed to induce mortality in adult mice of either strain. Detection results revealed that AKAV exclusively infected the brain tissue of the mice that died or were euthanized before the end of the experiment, primarily targeting neuronal cells. The infected brain tissues exhibited pathological changes including perivascular cuffing, microglial infiltration, neuronal degeneration/necrosis, vascular dilatation and congestion, etc.

The experimental mouse models and the lethal dose preliminarily explored in this study hold significant implications for vaccine/drug development and research on viral pathogenesis. For example, challenge-protection assays can be utilized to evaluate the efficacy of drug/vaccine candidates against AKAV infection, such as assessing their ability to reduce or eliminate mortality.

Acknowledgements
Not applicable.

Authors' contributions
JJ.W.: Conceptualization, methodology, formal analysis, writing—original draft preparation. RY.Y.and F.W.: investigation, methodology, formal analysis. DJ.C. and SQ.W.: supervision, funding acquisition, writing—review and editing. All authors reviewed the manuscript.

Funding
This work was supported by the National Key Research and Development Program of China (2022YFD18002000), the Fundamental Research Funds of Chinese Academy of Quality and Inspection & Testing (2024JK002), and the Beijing Natural Science Foundation (6254044).

Data availability
All data associated with this study are included in the paper. The AKAV strains mentioned in this study are available in GenBank (Table 4).

Declarations

Ethics approval and consent to participate
Animal studies were conducted following the guidelines of the experimental animal care and use guidelines of the Beijing Animal Control Committee. This experiment was approved by the Animal Welfare Ethics Committee of Beijing MDKN Biotechnology Co., LTD., with approval No. MDKN-2024–084. All efforts were made to minimize animal suffering.

Consent for publication
Not applicable.

Competing interests
The authors declare no competing interests.

Received: 23 April 2025 Accepted: 1 June 2025
Published online: 07 June 2025

References

1. Kirkland PD. Akabane virus infection. Rev Sci Tech. 2015;34(2):403–10. Available from: http://www.ncbi.nlm.nih.gov/entrez/query.fcgi?cmd=Retrieve&db=pubmed&dopt=Abstract&list_uids=26601444&query_hl=110.20506/rst.34.2.2366.
2. Yamakawa M, Yanase T, Kato T, Tsuda T. Chronological and geographical variations in the small rna segment of the teratogenic akabane virus. Virus Res. 2006;121(1):84–92. Available from: http://www.ncbi.nlm.nih.gov/entrez/query.fcgi?cmd=Retrieve&db=pubmed&dopt=Abstract&list_uids=16730837&query_hl=110.1016/j.virusres.2006.04.007.
3. Wang J, Firth C, Amos-Ritchie R, Davis SS, Yin H, Holmes EC, et al. Evolutionary history of simbu serogroup orthobunyaviruses in the australian episystem. Virology. 2019;535:32–44. Available from: http://www.ncbi.nlm.nih.gov/entrez/query.fcgi?cmd=Retrieve&db=pubmed&dopt=Abstract&list_uids=31261025&query_hl=110.1016/j.virol.2019.06.013.
4. Kono R, Hirata M, Kaji M, Goto Y, Ikeda S, Yanase T, et al. Bovine epizootic encephalomyelitis caused by akabane virus in southern japan. Bmc Vet Res. 2008;4:20. Available from: http://www.ncbi.nlm.nih.gov/entrez/query.fcgi?cmd=Retrieve&db=pubmed&dopt=Abstract&list_uids=18554406&query_hl=110.1186/1746-6148-4-20.
5. Oya AOTOT. Akabane, a new arbovirus isolated in japan. Jpn J Med Sci Biol. 1961;14:101–8.
6. Yanase T, Kato T, Hayama Y, Akiyama M, Itoh N, Horiuchi S, et al. Transition of akabane virus genogroups and its association with changes in the nature of disease in japan. Transbound Emerg Dis. 2018;65(2):e434-43. Available from: http://www.ncbi.nlm.nih.gov/entrez/query.fcgi?cmd=Retrieve&db=pubmed&dopt=Abstract&list_uids=29193771&query_hl=110.1111/tbed.12778.
7. Miyazato S, Miura Y, Hase M, Kubo M, Goto Y, Kono Y. Encephalitis of cattle caused by iriki isolate, a new strain belonging to akabane virus. Nihon Juigaku Zasshi. 1989;51(1):128–36. Available from: http://www.ncbi.nlm.nih.gov/entrez/query.fcgi?cmd=Retrieve&db=pubmed&dopt=Abstract&list_uids=2494374&query_hl=110.1292/jvms1939.51.128.
8. Uchida K, Murakami T, Sueyoshi M, Tsuda T, Inai K, Acorda JA, et al. Detection of akabane viral antigens in spontaneous lymphohistiocytic encephalomyelitis in cattle. J Vet Diagn Invest. 2000;12(6):518–24. Available from: http://www.ncbi.nlm.nih.gov/entrez/query.fcgi?cmd=Retrieve&db=pubmed&dopt=Abstract&list_uids=11108451&query_hl=110.1177/104063870001200605.
9. Kamata H, Inai K, Maeda K, Nishimura T, Arita S, Tsuda T, et al. Encephalomyelitis of cattle caused by akabane virus in southern japan in 2006. J Comp Pathol. 2009;140(2–3):187–93. Available from: http://www.ncbi.nlm.nih.gov/entrez/query.fcgi?cmd=Retrieve&db=pubmed&dopt=Abstract&list_uids=19162275&query_hl=110.1016/j.jcpa.2008.12.001.
10. Lee JK, Park JS, Choi JH, Park BK, Lee BC, Hwang WS, et al. Encephalomyelitis associated with akabane virus infection in adult cows. Vet Pathol. 2002;39(2):269–73. Available from: http://www.ncbi.nlm.nih.gov/entrez/query.fcgi?cmd=Retrieve&db=pubmed&dopt=Abstract&list_uids=12009066&query_hl=110.1354/vp.39-2-269.
11. Oem JK, Lee KH, Kim HR, Bae YC, Chung JY, Lee OS, et al. Bovine epizootic encephalomyelitis caused by akabane virus infection in korea. J Comp Pathol. 2012;147(2–3):101–5. Available from: http://www.ncbi.nlm.nih.gov/entrez/query.fcgi?cmd=Retrieve&db=pubmed&dopt=Abstract&list_uids=22520820&query_hl=110.1016/j.jcpa.2012.01.013.
12. Metselaar D, Robin Y. Akabane virus isolated in kenya. Vet Rec. 1976;99(5):86. Available from: http://www.ncbi.nlm.nih.gov/entrez/query.fcgi?cmd=Retrieve&db=pubmed&dopt=Abstract&list_uids=982784&query_hl=110.1136/vr.99.5.86-a.
13. Lee H, Jeong H, Park S, Yang M, Kim J, Bae J, et al. Experimental infection of cows with newly isolated akabane virus strain (akav-7) causing encephalomyelitis. Vet Res. 2016;47(1):62. Available from: http://www.ncbi.nlm.nih.gov/entrez/query.fcgi?cmd=Retrieve&db=pubmed&dopt=Abstract&list_uids=27287214&query_hl=110.1186/s13567-016-0349-6.
14. Jeong H, Oem J, Yang M, Yang D, Kim M, Lee K, et al. Experimental infection of goats with a newly isolated strain of akabane virus that causes encephalomyelitis. J Comp Pathol. 2017;157(2–3):220–9. Available from: http://www.ncbi.nlm.nih.gov/entrez/query.fcgi?cmd=Retrieve&db=pubmed&dopt=Abstract&list_uids=28673487&query_hl=110.1016/j.jcpa.2017.05.003.
15. Konno S, Moriwaki M, Nakagawa M. Akabane disease in cattle: congenital abnormalities caused by viral infection. Spontaneous disease Vet Pathol. 1982;19(3):246–66. Available from: http://www.ncbi.nlm.nih.gov/entrez/query.fcgi?cmd=Retrieve&db=pubmed&dopt=Abstract&list_uids=7200278&query_hl=110.1177/030098588201900304.
16. Ogawa Y, Fukutomi T, Sugiura K, Sugiura K, Kato K, Tohya Y, et al. Comparison of akabane virus isolated from sentinel cattle in japan. Vet Microbiol. 2007;124(1–2):16–24. Available from: http://www.ncbi.nlm.nih.gov/entrez/query.fcgi?cmd=Retrieve&db=pubmed&dopt=Abstract&list_uids=17467929&query_hl=110.1016/j.vetmic.2007.03.020.
17. Murata Y, Uchida K, Shioda C, Uema A, Bangphoomi N, Chambers JK, et al. Histopathological studies on the neuropathogenicity of the iriki and obe-1 strains of akabane virus in balb/cajcl mice. J Comp Pathol. 2015;153(2–3):140–9. Available from: http://www.ncbi.nlm.nih.gov/entrez/query.fcgi?cmd=Retrieve&db=pubmed&dopt=Abstract&list_uids=26184805&query_hl=110.1016/j.jcpa.2015.06.003.
18. Takenaka-Uema A, Matsugo H, Ohira K, Sekine W, Murakami S, Horimoto T. Different organ and tissue tropism between akabane virus genogroups in a mouse model. Virus Res. 2022;314:198752. Available from: http://www.ncbi.nlm.nih.gov/entrez/query.fcgi?cmd=Retrieve&db=pubmed&dopt=Abstract&list_uids=35331837&query_hl=110.1016/j.virusres.2022.198752.
19. Chen D, Wang D, Wei F, Kong Y, Deng J, Lin X, et al. Characterization and reverse genetic establishment of cattle derived akabane virus in china. Bmc Vet Res. 2021;17(1):349. Available from: http://www.ncbi.nlm.nih.gov/entrez/query.fcgi?cmd=Retrieve&db=pubmed&dopt=Abstract&list_uids=34781948&query_hl=110.1186/s12917-021-03054-x.
20. Chen D, Wang J, Wei F, Jing H, Wang D, Zhang Z, et al. Characterization and double-antibody sandwich elisa application of a monoclonal antibody against akabane virus nucleocapsid protein. J Aoac Int.

2023;106(4):931–8. Available from: http://www.ncbi.nlm.nih.gov/entrez/query.fcgi?cmd=Retrieve&db=pubmed&dopt=Abstract&list_uids=36782359&query_hl=110.1093/jaoacint/qsad025.
21. Wang J, Chen D, Wei F, Deng J, Su J, Lin X, et al. Generation of stable cell lines expressing akabane virus n protein and insight into its function in viral replication. Pathogens. 2023;12(8):1058. Available from: http://www.ncbi.nlm.nih.gov/entrez/query.fcgi?cmd=Retrieve&db=pubmed&dopt=Abstract&list_uids=37624018&query_hl=110.3390/pathogens12081058.
22. Reed LJ, Muench H. A simple method of estimating fifty per cent endpoints. Am J Epidemiol. 1938;27(3):493–7. https://doi.org/10.1093/oxfordjournals.aje.a118408.
23. Meng J, He Y, Li N, Yang Z, Fu S, Wang D, et al. Akabane virus isolated from biting midges and its infection in local domestic animal, yunnan, china: a field and laboratory investigation. Front Cell Infect Microbiol. 2024;14:1434045. Available from: http://www.ncbi.nlm.nih.gov/entrez/query.fcgi?cmd=Retrieve&db=pubmed&dopt=Abstract&list_uids=39897479&query_hl=110.3389/fcimb.2024.1434045.
24. Gao H, Wang J, Yang Z, Xie J, He Y, Hong Q, et al. Genetic and pathogenic characterisation of a virulent akabane virus isolated from goats in yunnan, china. J Vet Res. 2022;66(1):35–42. Available from: http://www.ncbi.nlm.nih.gov/entrez/query.fcgi?cmd=Retrieve&db=pubmed&dopt=Abstract&list_uids=35582486&query_hl=110.2478/jvetres-2022-0007.
25. Na E, Jeong C, Chae S, Oem J. Investigating the reassortment potential and pathogenicity of the s segment in akabane virus using a reverse genetics system. Bmc Vet Res. 2025;21(1):20. Available from: http://www.ncbi.nlm.nih.gov/entrez/query.fcgi?cmd=Retrieve&db=pubmed&dopt=Abstract&list_uids=39815297&query_hl=110.1186/s12917-024-04459-0.
26. Vorbrodt AW, Lossinsky AS, Wisniewski HM. Localization of alkaline phosphatase activity in endothelia of developing and mature mouse blood-brain barrier. Dev Neurosci. 1986;8(1):1–13. Available from: http://www.ncbi.nlm.nih.gov/entrez/query.fcgi?cmd=Retrieve&db=pubmed&dopt=Abstract&list_uids=3743466&query_hl=110.1159/000112236.
27. Ishihara Y, Shioda C, Bangphoomi N, Sugiura K, Saeki K, Tsuda S, et al. Akabane virus nonstructural protein nsm regulates viral growth and pathogenicity in a mouse model. J Vet Med Sci. 2016;78(9):1391–7. Available from: http://www.ncbi.nlm.nih.gov/entrez/query.fcgi?cmd=Retrieve&db=pubmed&dopt=Abstract&list_uids=27181086&query_hl=110.1292/jvms.16-0140.
28. Konno S, Nakagawa M. Akabane disease in cattle: congenital abnormalities caused by viral infection. Experimental disease. Vet Pathol. 1982;19(3):267–79. Available from: http://www.ncbi.nlm.nih.gov/entrez/query.fcgi?cmd=Retrieve&db=pubmed&dopt=Abstract&list_uids=7200279&query_hl=110.1177/030098588201900305.
29. Oem J, Yoon H, Kim H, Roh I, Lee K, Lee O, et al. Genetic and pathogenic characterization of akabane viruses isolated from cattle with encephalomyelitis in korea. Vet Microbiol. 2012;158(3–4):259–66. Available from: http://www.ncbi.nlm.nih.gov/entrez/query.fcgi?cmd=Retrieve&db=pubmed&dopt=Abstract&list_uids=22464491&query_hl=110.1016/j.vetmic.2012.02.017.
30. Marin-Lopez A, Calvo-Pinilla E, Moreno S, Utrilla-Trigo S, Nogales A, Brun A, et al. Modeling arboviral infection in mice lacking the interferon alpha/beta receptor. Viruses. 2019;11(1):35. Available from: http://www.ncbi.nlm.nih.gov/entrez/query.fcgi?cmd=Retrieve&db=pubmed&dopt=Abstract&list_uids=30625992&query_hl=110.3390/v11010035.
31. Beer M, Conraths FJ, van der Poel WHM. 'schmallenberg virus'–a novel orthobunyavirus emerging in europe. Epidemiol Infect. 2013;141(1):1–08. Available from: http://www.ncbi.nlm.nih.gov/entrez/query.fcgi?cmd=Retrieve&db=pubmed&dopt=Abstract&list_uids=23046921&query_hl=110.1017/S0950268812002245.
32. Wernike K, Breithaupt A, Keller M, Hoffmann B, Beer M, Eschbaumer M. Schmallenberg virus infection of adult type i interferon receptor knockout mice. Plos One. 2012;7(7):e40380. Available from: http://www.ncbi.nlm.nih.gov/entrez/query.fcgi?cmd=Retrieve&db=pubmed&dopt=Abstract&list_uids=22792298&query_hl=110.1371/journal.pone.0040380.
33. Boshra HY, Charro D, Lorenzo G, Sanchez I, Lazaro B, Brun A, et al. Dna vaccination regimes against schmallenberg virus infection in ifnar(-/-) mice suggest two targets for immunization. Antiviral Res. 2017;141:107–15. Available from: http://www.ncbi.nlm.nih.gov/entrez/query.fcgi?cmd=Retrieve&db=pubmed&dopt=Abstract&list_uids=28235558&query_hl=110.1016/j.antiviral.2017.02.013.
34. Boshra H, Lorenzo G, Charro D, Moreno S, Guerra GS, Sanchez I, et al. A novel schmallenberg virus subunit vaccine candidate protects ifnar(-/-) mice against virulent sbv challenge. Sci Rep. 2020;10(1):18725. Available from: http://www.ncbi.nlm.nih.gov/entrez/query.fcgi?cmd=Retrieve&db=pubmed&dopt=Abstract&list_uids=33230115&query_hl=110.1038/s41598-020-73424-2.
35. Na E, Chae S, Oh B, Jeong C, Park S, Oem J. A novel approach using ifnar1 ko mice for assessing akabane virus pathogenicity and vaccine efficacy. Vaccine. 2025;53:127094. Available from: http://www.ncbi.nlm.nih.gov/entrez/query.fcgi?cmd=Retrieve&db=pubmed&dopt=Abstract&list_uids=40209629&query_hl=110.1016/j.vaccine.2025.127094.

Publisher's Note